POLSKA AKADEMIA NAUK

INSTYTUT MASZYN PRZEPŁYWOWYCH

TRANSACTIONS OF THE INSTITUTE OF FLUID-FLOW MACHINERY

PRACE INSTYTUTU MASZYN PRZEPŁYWOWYCH

103

GDAŃSK 1997

THE TRANSACTIONS OF THE INSTITUTE OF FLUID-FLOW MACHINERY

exist for the publication of theoretical and experimental investigations of all aspects of the mechanics and thermodynamics of fluid-flow with special reference to fluid-flow machines

*

PRACE INSTYTUTU MASZYN PRZEPŁYWOWYCH

poświęcone są publikacjom naukowym z zakresu teorii i badań doświadczalnych w dziedzinie mechaniki i termodynamiki przepływów, ze szczególnym uwzględnieniem problematyki maszyn przepływowych

Wydanie publikacji dofinansowane zostało przez PAN ze środków DOT uzyskanych z Komitetu Badań Naukowych

EDITORIAL OFFICE – REDAKCJA

Wydawnictwo Instytutu Maszyn Przepływowych
Polskiej Akademii Nauk
ul. Gen. Józefa Fiszera 14, 80-952 Gdańsk, skr. poczt. 621,
☎ (0-58) 46-08-81 wew. 141, fax: (0-58) 41-61-44,
e-mail: esli@imppan.imp.pg.gda.pl

ISSN 0079-3205

TRANSACTIONS OF THE INSTITUTE OF FLUID-FLOW MACHINERY

1997 No. 103

JAROSŁAW MIKIELEWICZ,[1] DARIUSZ MIKIELEWICZ[2]

Semi-analytical model of spray impingement on a flat surface[3]

Two-phase flow of air and small droplets impinging normally on a plate has been considered. The problem has been postulated in such a form that it is possible to obtain an analytical solution for the trajectory of the droplet. Solutions in radial and longitudinal directions are independent from each other. The air flow is determined by a potential flow. The drop paths are determined from consideration of the force balance on a droplet. As long as viscous effects can be neglected the analytical solution is exac but when viscous effects start to play an important role the numerical integration of postulated equations is required.

Nomenclature

a – nozzle coefficient in equation (6),
C_x – friction coefficient,
C_i – integration constants,
d – droplet diameter,
D – nozzle diameter,
g – mass concentration, $\dot{m}_k/\dot{V}_g$,
H – height of nozzle suspension over the surface,
$\dot{m}$ – mass flow rate of liquid,
p – radial co-ordinate in r direction (boundary condition),
q – vertical velocity in z direction (initial condition),
r, z – cylindrical co-ordinates,
s – beginning of integration in z direction (initial condition),
Stk – Stokes number, $u_d \rho d_k^2/(18\mu_g H)$,
t – time,
u – radial velocity,
v – longitudinal velocity,
$\dot{V}$ – volumetric flow rate of gas,
δ – liquid layer thickness,
η – non-dimensional distance,
μ – dynamic viscosity,
ρ – liquid density,
τ – wall shear stress.

Subscripts

d – nozzle,
g – gas, concentration,
k – droplet,
l – liquid,
r – radial direction,
z – perpendicular direction to the surface,
u – velocity,
w – wall.

[1]Institute of Fluid-Flow Machinery, Department of Thermodynamics and Heat Transfer, Fiszera 14, 80-952 Gdańsk

[2]Technical University of Gdańsk, Faculty of Mechanical Enginnering,Narutowicza 11/12, 80-952 Gdańsk

[3]The paper was funded by a research project KBN 3P404 034 07

Superscripts

$+$ – non-dimensional quantity.

1. Introduction

Cooling of hot surfaces by sprays can be found in a number of industrial processes. Evaporation of drops on a hot surface can considerably enhance the rate of heat removal from that surface and makes this type of heat removal much more efficient when compared with that caused by air flow at otherwise identical conditions. The mist flow is much more economic than the single liquid flow because it requires less liquid and therefore is more economically sound. A number of existing studies [1-8] present various aspects of the considered phenomenon. So far there is a lack of a comprehensive theoretical model that would allow for reliable predictions of the whole process of spray cooling. Up to date only some empirical correlations describing hydrodynamics and heat transfer of two phase jets have been suggested, but the conditions and precise parametric regions of applicability of these expressions are by no means firmly established. Theoretical concepts are usually too simple to properly describe the problem or too complex to be recommended for general applications.

In the paper, the hydrodynamics of an axisymmetric spray jet falling normally onto a horizontal plate is studied. During the impingement of a gas atomised spray the drops having relatively higher inertia deviate from the air streamlines before they hit the surface. The mist flow is presumed to be diluted enough in order to ignore the interaction between the droplets. The surface during the process remains almost dry. The impinging droplets are either elastically dispersed or captured by a surface. The model derived in this work has solid theoretical basis and moreover the analytical solution of this problem is given. The model is based on consideration of inertial forces acting on a droplet whereas gas motion is governed by the potential flow.

2. Theoretical model of two-phase spray

The flow pattern in a spray is shown schematically in Fig. 1. The flow of air outside the jet is assumed to be stagnant and the only flow is created by an axisymmetric jet impinging normally on a flat plate. Axisymmetric jet can be subdivided into three characteristic regions: the free jet region, the stagnation flow region and the region of radial flow outside the stagnation zone called the wall region. The flow becomes sensitive to the presence of the plate only within the wall region and postulated model is valid only in this region. The air stream exiting the nozzle has a nearly rectangular velocity profile. As the air jet traverses the ambient air its boundary spreads and widens. For the sufficient length of the free jet the velocity distribution approaches a bell-shape, which can be described approximately by a Gaussian distribution. The effects of stagnation are experienced in the vicinity of the surface (approximately one to two times the nozzle diameter in the longitudinal direction). In this region the vertical velocity component is decelerated and is transformed into an accelerated horizontal one.

The wall region is commonly believed to begin at the distance $x = 5D$ from

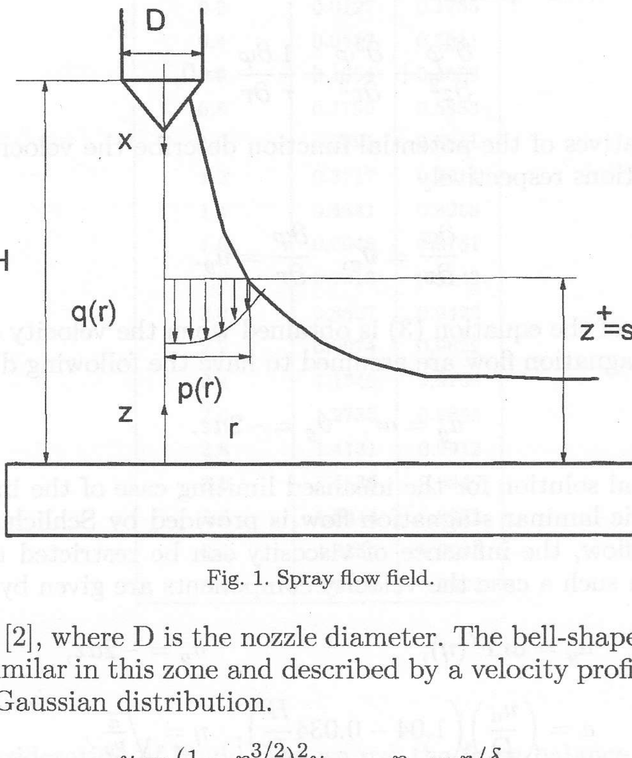

Fig. 1. Spray flow field.

the nozzle exit [2], where D is the nozzle diameter. The bell-shape velocity distribution is self similar in this zone and described by a velocity profile which closely resembles the Gaussian distribution.

$$u = (1 - \eta_u^{3/2})^2 u_m, \quad \eta_u = r/\delta_u, \tag{1}$$

where

$$u_m = 8(3 + 0.85x/D)^{-1} u_d,$$

$$\delta_u = 0.20x.$$

Similarly, the droplet concentration distribution is given in the form:

$$g = (1 - \eta_g^{3/2})^2 g_m, \quad \eta_g = r/\delta_g, \tag{2}$$

where

$$g_m = 8(3 + 0.85x/D)^{-1} g_d,$$

$$\delta_g = 0.14x.$$

The velocity and concentration compents of the ideal stagnant flow are provided by Buyevich et al. [2].

2.1. Gas flow

In the considered problem of a two-phase spray the air flow is described by the following potential equation

$$\frac{\partial^2 \varphi}{\partial z^2} + \frac{\partial^2 \varphi}{\partial r^2} + \frac{1}{r}\frac{\partial \varphi}{\partial r} = 0, \tag{3}$$

where the derivatives of the potential function describe the velocity components in r and z directions respectively

$$\frac{\partial \varphi}{\partial z} = \vartheta_g, \qquad \frac{\partial \varphi}{\partial r} = u_g. \tag{4}$$

The solution of the equation (3) is obtained when the velocity components of axisymmetric stagnation flow are assumed to have the following distributions

$$u_g = ar, \quad \vartheta_g = -2az. \tag{5}$$

The analytical solution for the idealised limiting case of the infinitely extended axisymmetric laminar stagnation flow is provided by Schlichting [3]. In the boundary layer flow, the influence of viscosity can be restricted to a thin layer near the wall. In such a case the velocity components are given by [2-3].

$$\begin{gathered} u_g = arF'(\eta), \qquad \vartheta_g = -2az, \\ a = \left(\frac{u_d}{D}\right)\left(1.04 - 0.034\frac{H}{D}\right), \quad \eta = \sqrt{\frac{a}{\nu_g}}\,. \end{gathered} \tag{6}$$

It can be checked by substitution of relevant values that the range of validity of the expression for a is for the values of H/D between 0 and 30.5. It is shown in Table 1 that for the distance from the wall approximately equal to $\eta = 2.4$ we have $F'(\eta) \approx 0.98$. If we consider the corresponding distance from the wall denoted as $z = \delta$, as the boundary layer, we have $\delta = 2.4\sqrt{\frac{\nu_g}{a}}$. Within this region we would have to include the viscous effects.

In the present analysis we assume:

- in the air jet there is a small fraction of drops,
- the drops do not affect the air flow,
- the flow of air is incompressible and inviscous; this assumption is obeyed provided the flow of air should not exceed 60 m/s (Mach number less than 0.2),
- the flow of air is potential within the jet,
- physical properties are temperature independent.

Table 1.

$\eta = z\sqrt{a/\nu}$	F	F'
0.0	0.0000	0.0000
0.2	0.0127	0.1755
0.4	0.0487	0.3311
0.6	0.1054	0.4669
0.8	0.1799	0.5833
1.0	0.2695	0.6811
1.2	0.3717	0.7614
1.4	0.4841	0.8258
1.6	0.6046	0.8761
1.8	0.7313	0.9142
2.0	0.8627	0.9422
2.2	0.9974	0.9622
2.4	1.1346	0.9760
2.6	1.2733	0.9853
2.8	1.4131	0.9912
3.0	1.5536	0.9949
3.2	1.6944	0.9972
3.4	1.8356	0.9985
3.6	1.9769	0.9992

2.2. Liquid flow

For the consideration of liquid flow we use the force balance on the droplet, see Fig. 2. In the stagnation region of the air flow, the droplet motion is calculated using the following momentum balance in r and z directions:

$$m_k \frac{du_k}{dt} = -F \cos\alpha, \tag{7}$$

$$m_k \frac{d\vartheta_k}{dt} = F \sin\alpha. \tag{8}$$

In the above equation F represents the resistance force acting on the droplet as a result of the droplet motion through air. This force can be expressed as:

$$F = C_x \frac{\rho_g}{2} A_k w^2, \qquad w^2 = \left[\left(u_k - u_g\right)^2 + \left(\vartheta_k - \vartheta_g\right)^2\right]. \tag{9}$$

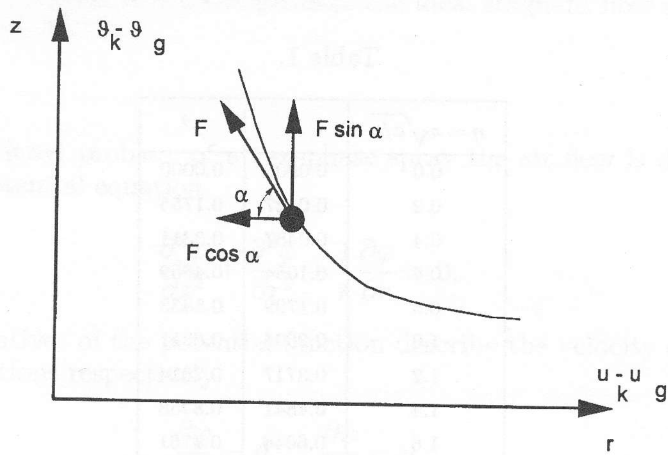

Fig. 2. Force balance on a droplet.

From Fig. 2 it can be seen that trigonometric functions appearing in equations (7) and (8) are defined as:

$$\cos\alpha = \frac{u_k - u_g}{\sqrt{(u_k-u_g)^2 + (\vartheta_k - \vartheta_g)^2}},$$
$$\sin\alpha = \frac{\vartheta_k - \vartheta_g}{\sqrt{(u_k-u_g)^2 + (\vartheta_k - \vartheta_g)^2}}. \tag{10}$$

Defining the droplet mass and surface area as

$$m_k = \rho_k \frac{\pi d_k^3}{6}, \quad A_k = \frac{\pi d_k^2}{4}, \tag{11}$$

and substituting for the skin friction coefficient,

$$C_x = \frac{24}{Re} = \frac{24\mu_g}{w d_k \rho_g}, \tag{12}$$

which is valid for small droplets in laminar flow, we obtain the following forms of droplet momentum balance equations

$$\frac{du_k}{dt} = -\frac{18\mu_g}{\rho_k d_k^2}\Big(u_k - u_g\Big),$$
$$\frac{d\vartheta_k}{dt} = \frac{18\mu_g}{\rho_k d_k^2}\Big(\vartheta_k - \vartheta_g\Big), \tag{13}$$

which reflects that the only forces acting on a droplet are the Stokes forces. Expressing the velocities as the derivatives of time we obtain:

$$\frac{d^2r}{dt^2} = -\frac{18\mu_g}{\rho_k d_k^2}\left(\frac{dr}{dt} - ar\right),$$
$$\frac{d^2z}{dt^2} = \frac{18\mu_g}{\rho_k d_k^2}\left(\frac{dz}{dt} + 2az\right). \tag{14}$$

The above equations are independent from each other and can be solved separately. Before solving these equations we introduce the non-dimensional variables:

$$t^+ = \frac{u_d t}{H},\quad r^+ = \frac{r}{H},\quad z^+ = \frac{z}{H},\quad a^+ = \frac{aH}{u_d},\quad K^+ = \frac{1}{Stk} = \frac{18\mu_g}{\rho_k d_k^2}\frac{H}{u_d}. \tag{15}$$

The general form of equations (14) is then obtained:

$$\frac{d^2r^+}{dt^{+2}} + K^+\frac{dr^+}{dt^+} - K^+a^+r^+ = 0,$$
$$\frac{d^2z^+}{dt^{+2}} + K^+\frac{dz^+}{dt^+} - 2K^+a^+z^+ = 0. \tag{16}$$

The following boundary conditions apply to the above set of equations:
Horizontal motion

$$\text{for}\quad t^+ = 0,\ r^+ = p,\ u^+ = 0. \tag{17}$$

Vertical motion

$$\text{for}\quad t^+ = 0,\ z^+ = s,\ \vartheta^+ = q(r). \tag{18}$$

In equation (17) p is a radial location of the droplet at the beginning of integration in the plane $z^+ = s$ (beginning of the wall jet region) and s is a corresponding vertical position of the beginning of integration. The quantity $q(r)$ is the initial velocity in vertical direction at the position $z^+ = s$. The general solution to the equations (16) can be found in the form

$$r^+(t)^+ = C_1 \exp\left[-\tfrac{1}{2}\left(K^+ + \sqrt{K^+(K^+ + 4a^+)}\right)t^+\right] +$$
$$+ C_2 \exp\left[-\tfrac{1}{2}\left(K^+ - \sqrt{K^+(K^+ + 4a^+)}\right)t^+\right], \tag{19}$$

where

$$C_1 = -\frac{1}{2}\frac{p\left(K^+ - \sqrt{K^+(K^+ + 4a^+)}\right)}{\sqrt{K^+(K^+ + 4a^+)}},$$
$$C_2 = \frac{1}{2}\frac{p\left(K^+ + \sqrt{K^+(K^+ + 4a^+)}\right)}{\sqrt{K^+(K^+ + 4a^+)}}, \tag{20}$$

and

$$z^+(t)^+ = C_3 \exp\left[\frac{1}{2}\left(K^+ + \sqrt{K^+(K^+ + 8a^+)}\right)t^+\right] + \\ + C_4 \exp\left[\frac{1}{2}\left(K^+ - \sqrt{K^+(K^+ + 8a^+)}\right)t^+\right], \tag{21}$$

where

$$C_3 = -\frac{1}{2}\frac{\left(K^+ s - \sqrt{K^+(K^+ + 8a^+)}\right) - 2q}{\sqrt{K^+(K^+ + 8a^+)}},$$
$$C_4 = \frac{1}{2}\frac{\left(K^+ s + \sqrt{K^+(K^+ + 8a^+)}\right) - 2q}{\sqrt{K^+(K^+ + 8a^+)}}. \tag{22}$$

These equations are valid up to the point where viscous effects start to dominate i.e. boundary layer where, as it was said before, the numerical integration of the above equations is required with inclusion of viscous effects. We will confine our analysis of the droplet motion to the point where the droplet will touch the boundary layer, i.e. $\delta = 2.4\sqrt{\frac{a}{\nu}}$. This is equivalent to neglecting viscous effects. As the thickness of boundary is very small we can to this and extend the inviscous zone onto the wall. Also, this is a good assumption because it should be noted that each droplet must have some vertical velocity in order to land. Additionally, if there is heating from the surface, the droplets will encounter some resistance from vapour created during evaporation of droplets. Hence, in our assumption this means that when a droplet has reached the boundary layer it will land and the radial position of landing will be the same as that of touching the boundary layer.

3. Results

Calculations to illustrate the validity of the model have been performed for different Stokes numbers ranging from 0.5 to 100 and also by taking H/D ratio to be 5 and 10. Varying H/D corresponds to varying the height of the nozzle suspension over the wall. The results are presented in Figs. 3 to 6. In the figures below r is a radial location of the droplet landing position and r_0 is a corresponding position at the start of integration of the droplet trajectory, r^* is a total jet radius at the start of integration ($z^+ = s$). In Figs. 3 and 4, there is presented the dependence of the radius of impingement with respect to the radius of the jet at the beginning of the wall-jet region. The result confirm the experimental observations where the higher the Stokes number (larger droplets) the landing radius of the jet containing droplets is smaller. The difference between various Stokes number calculations are not significant especially for $Stk > 5$, where the results overlap. Another observation is that the distributions of r are almost linear with respect to r_0, except for the first case of $Stk = 0.5$. When the ratio H/D is increased the differences between the landing radius for different Stokes number predictions are smaller.

The second aspect on which the attention was focused was the dependence of impact velocity on the radius of the impact. These are presented in Figs. 5 and 6. The obvious trends are confirmed by the solution. The impact velocity decreases as the Stokes number increases and with increasing H/D ratio the overall reduction in relative values of impact velocity is observed.

Then the attention was focused to the droplet concentration on the plate. This has a significant practical importance, because this is a measure of heat required for complete evaporation of the stream of droplets. Concentration at the beginning of integration, g_0, was initially calculated from Gaussian distribution (eqn. (2)) but at the impact plane it was calculated from the evident mass balance of droplets for an element slice of the profile of concentration at the beginning of integration and at the impact plane. This balance is conserved at the beginning of integration and on the plane of impact.

$$\Delta \dot{m}_k = 2\pi\, g_0\, \vartheta_0\, \rho_k\, r, \qquad \Delta r = 2\pi\, g\, \vartheta\, rho_k\, r_1\, \Delta\, r_1, \tag{23}$$

and then

$$g = g_0 \left(\frac{\vartheta_0}{\vartheta}\right)\left(\frac{r_0}{r}\right)\left(\frac{\Delta r_0}{\Delta r}\right). \tag{24}$$

The graphs presenting the dependence of normalised liquid concentration (with respect to concentration at the beginning of zone) as a function of the radius of impact are presented in Fig. 7 and 8. Finally, in Fig. 9 presented is the dependence of maximum radius of impact normalised by the radius at the start of wall jet region r^* (radius envelope) as a function of Stokes number at different values of H/D.

4. Conclusions

An analytical model of spray impingement on a flat surface has been developed. The model considers the influence of droplet inertial forces on their trajectory. Therefore it is a rather good approximation of the phenomenon for small

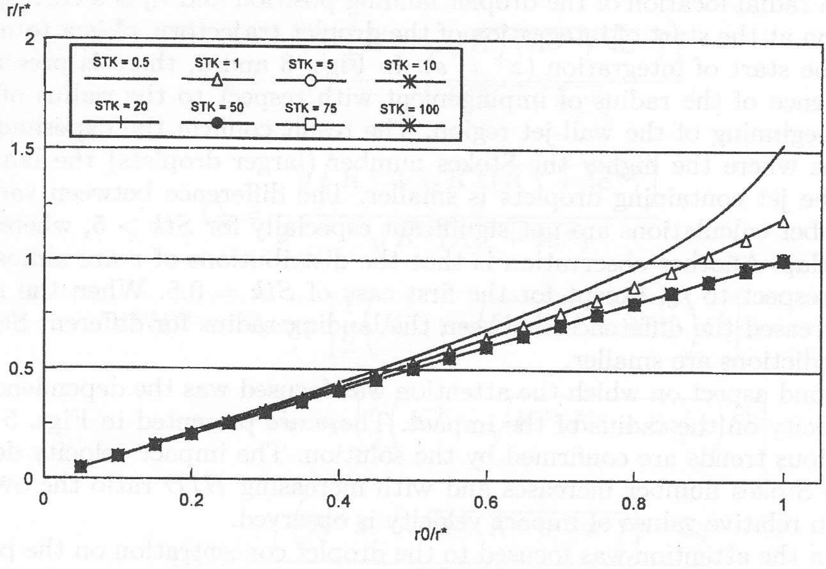

Fig. 3. Dependence of radius of impact for $H/D = 5$.

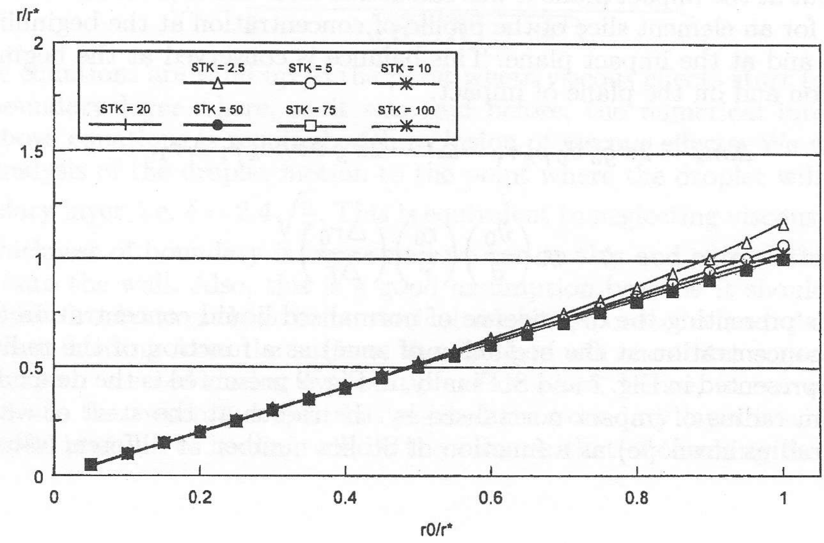

Fig. 4. Dependence of radius of impact for $H/D = 10$.

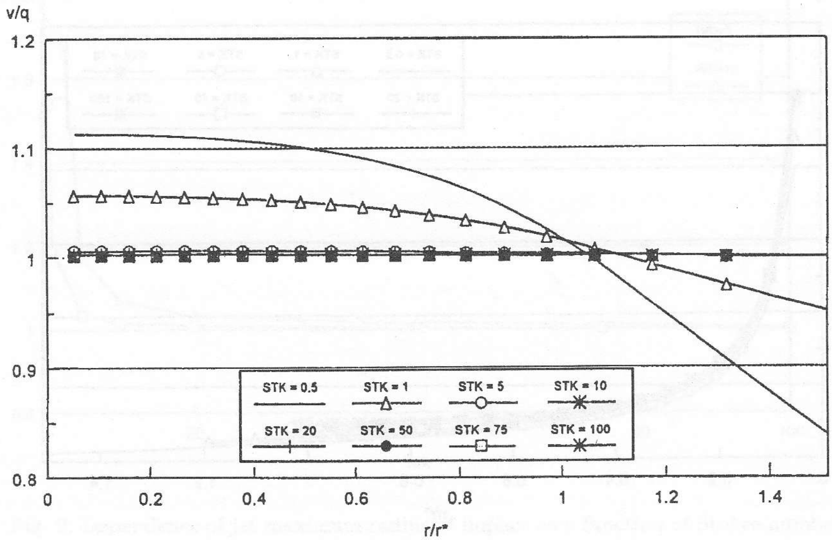

Fig. 5. Dependence of dimensionless droplet impact velocity on the radius of impact, $H/D = 5$.

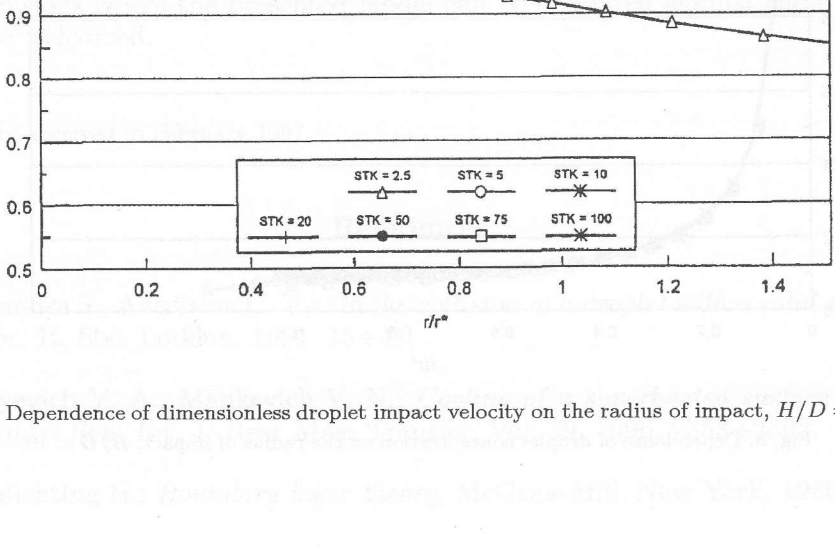

Fig. 6. Dependence of dimensionless droplet impact velocity on the radius of impact, $H/D = 10$.

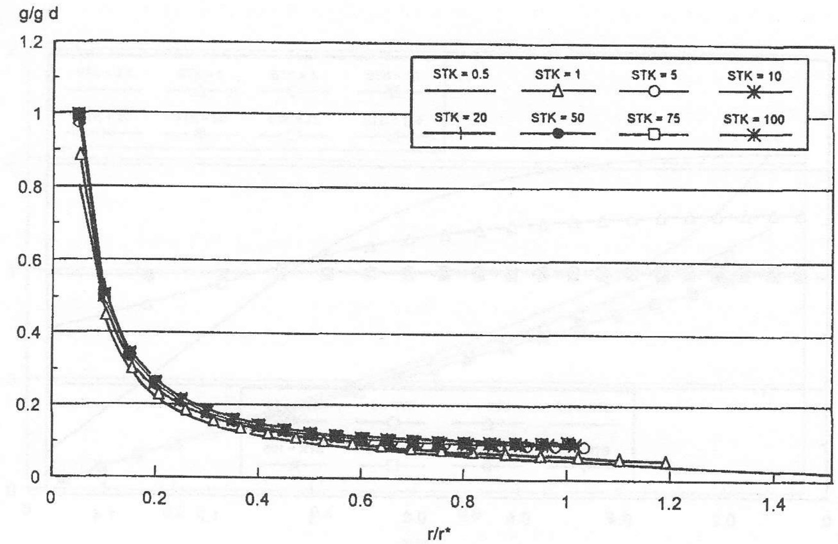

Fig. 7. Dependence of droplet concentration on the radius of impact, $H/D = 5$.

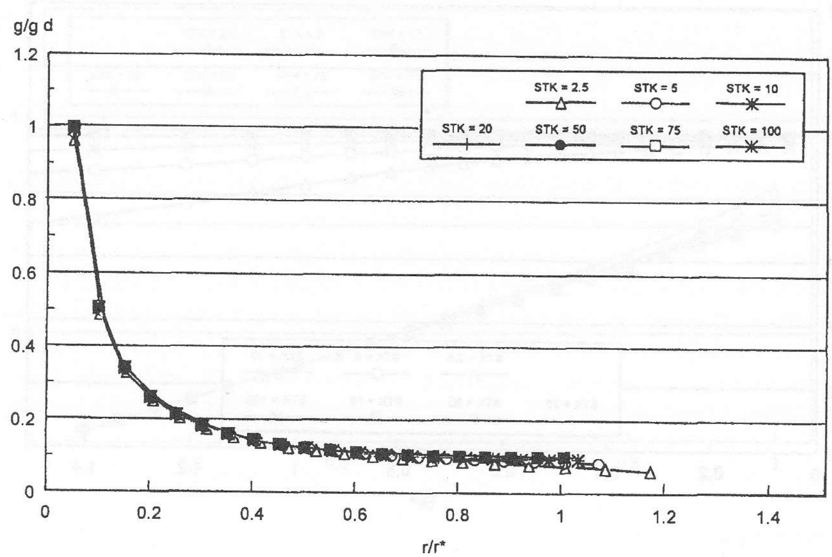

Fig. 8. Dependence of droplet concentration on the radius of impact, $H/D = 10$.

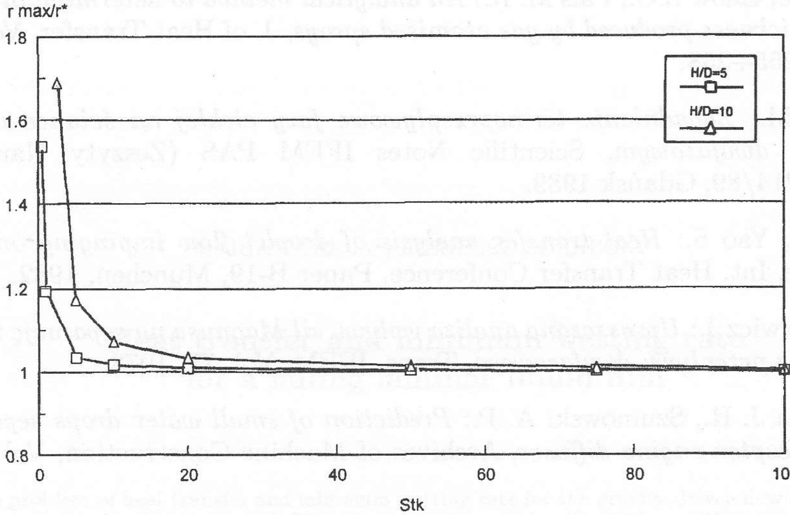

Fig. 9. Dependence of jet maximum radius of impact as a function of Stokes number.

droplets intensively penetrating the stagnant flow. The solutions of ordinary differential equations describing the problem are independent from each other in both radial and longitudinal directions. Calculations of droplet radius of impact and impact velocity as a function of impact radius confirm good behaviour of the model with observed experimental trends. These are, however, very difficult to obtain as usually other parameters are studied. Calculated have also been the droplet concentrations on a plate. With the aid of the above solution various testing and validation of existing computer codes can be conducted. Carefully conducted experiments for obtaining impact velocities, droplet trajectories and concentrations where the presented model can be validated against these values would be welcomed.

Manuscript received in February 1997

References

[1] Chandra S., Avedisian C. T.: *On the collision of a droplet with a solid surface*, Proc. R. Soc. London, 1991, 15÷41.

[2] Buyevich Y. A., Mankevich V. N.: *Cooling of a superheated surface with a jet mist flow*, Int. J. Heat Mass Transfer, Vol. 39, 1996, 2353÷2362.

[3] Schlichting H.: *Boundary layer theory*, McGraw-Hill, New York, 1980.

[4] Yang J., Chow L.C., Pais M. R.: *An analytical method to determine the liq film thickness produced by gas atomised sprays*, J. of Heat Transfer, Vol. 11 1996, 255÷258.

[5] Trela M.: *Zagadnienia termoprzepływowe fazy ciekłej na ściance w prz pływie dwufazowym*, Scientific Notes IFFM PAS (Zeszyty Naukowe) 293/1214/89, Gdańsk 1989.

[6] Liu L., Yao S.: *Heat transfer analysis of droplet flow impinging on a ho surface*, Int. Heat Transfer Conference, Paper B-19, Munchen, 1982.

[7] Mikielewicz J.: *Uproszczona analiza wpływu sił Magnusa na separację małyc kropel z przepływu dwufazowego*, Trans. IFFM, Vol. 75, 1978.

[8] Piechna J. R., Szumowski A. P.: *Prediction of small water drops separatio in helicopter engine diffuser*, Archives of Machine Construction, Vol. XLII, 1995.

[9] Martin H.: *Heat and mass transfer between impinging gas jets and solid sur-faces*, Advances in Heat Transfer, Vol. 13, 1977, 1÷60.

Półanalityczny model rozpływu strugi dwufazowej na płaskiej powierzchni

Streszczenie

W pracy rozpatrzono napływ dwufazowy powietrza i małych kropelek na płaską powierzchnię. Roz-wiązanie zadania zostało przedstawione w sposób analityczny, podając ruch kropli w kierunku pionowym i poziomym. Przepływ powietrza jest przepływem potencjalnym natomiast ruch kropel rozwiązywany jest z bilansu sił dla poszczególnych kropli. Przedstawiony model zjawiska obowiązuje dla przepływów, gdzie efekty lepkościowe są do pominięcia, tzn. poza warstwą przyścienną.